

Excitation mechanism of standing waves produced by electron beam plasma instability

N. Hayashi, M. Tanaka, S. Shinohara, and Y. Kawai

Interdisciplinary Graduate School of Engineering Sciences, Kyushu University, Kasuga, Fukuoka 816, Japan

(Received 17 April 1995; accepted 5 July 1995)

The excitation mechanism of standing waves produced by the electron beam plasma instability is experimentally studied using a Double Plasma device. When an electron beam is injected into the target plasma, standing waves around the electron plasma frequency are excited. A test wave is propagated in an electron beam plasma system and is identified as the beam mode from the dispersion relation. The propagation direction of the beam mode is determined from the wave pattern utilizing a phase shifter. It is found that a reflected beam mode exists as well as a forward beam mode, and is generated by the reflection of the forward beam mode from a potential well produced by the injection of the electron beam. The observed standing waves are formed by superposing the beam modes propagating in opposite directions from each other. © 1995 American Institute of Physics.

I. INTRODUCTION

When an electron beam is injected into a plasma, unstable waves around the electron plasma frequency are excited by the electron beam plasma instability.¹⁻⁷ The dispersion relation of this instability is written as follows:⁸

$$\frac{\omega_{pe}^2}{\omega^2 - \frac{3}{2}k^2v_{the}^2} + \frac{\omega_{pb}^2}{(\omega - ku)^2} = 1, \quad (1)$$

where $\omega_{pe} (= (4\pi n_e e^2/m_e)^{1/2})$ and $\omega_{pb} (= (4\pi n_b e^2/m_e)^{1/2})$ are the plasma frequency of bulk electrons and an electron beam, respectively. Here v_{the} and u are the electron thermal velocity and the electron beam velocity, and n_e and n_b are the density of bulk electrons and electron beam, respectively. As is well known, the electron beam plasma instability derived from Eq. (1) is the convective instability,⁸ namely, unstable waves spatially grow. In most of the experiments on the electron beam plasma instability, unstable waves have been observed¹ as a traveling wave. On the other hand, there are some cases⁹⁻¹⁷ where standing waves are observed between the boundary in a plasma. Looney and Brown¹³ observed standing waves between two electrodes in a glass tube discharge plasma, where the waves did not grow or damp spatially. The standing wave patterns which they found were theoretically explained by Sumi¹⁴ using Eq. (1). Kawabe¹⁵ also obtained results similar to those of Looney and Brown. Furthermore, he observed fine structures of the electron plasma oscillation and the higher harmonics. Roberson *et al.*^{16,17} excited standing waves by inserting a grid in an electron beam plasma column, and measured the reflection coefficients of the electron plasma wave propagating into a density gradient.

A standing wave is generally formed by superposing a forward wave and a reflected one. Usually positive feedback is necessary for the excitation of unstable waves with standing wave patterns. Internal feedback transmitted in a plasma or external feedback transmitted through external circuits is considered as positive feedback. However, this feedback mechanism, which is one of the most fundamental processes

in the electron beam plasma instability, has not been studied so far. When internal positive feedback takes place, unstable waves are reflected at a boundary and propagate oppositely in the plasma. So, it is very important to examine the propagation direction of unstable waves. The reflected wave damps if there is not a reflected electron beam, so that the reflected electron beam which is necessary for the excitation of the instability should exist. Thus, it is crucial for understanding the mechanism of positive feedback in an electron beam plasma system to measure the reflected electron beam.

In this paper, we excited the electron beam plasma instability whose wave number takes discrete values, namely, the standing wave and clarified its generation mechanism by measuring the energy distribution functions of electrons as well as the dispersion relation of the instability. Furthermore, we measured the propagation direction with a phase shifter. It is the first time, to our knowledge, to have confirmed the existence of both a reflected electron beam and a reflected beam mode. In Sec. II, the experimental apparatus is described. The experimental results and discussion are given in Sec. III. Conclusions are summarized in Sec. IV.

II. EXPERIMENTAL APPARATUS

Figure 1 shows a schematic diagram of the experimental apparatus. Double Plasma (D.P.) device dimensions were 120 cm in axial length and 70 cm in diameter. The chamber was evacuated to 3×10^{-7} Torr, and then argon gases were introduced into the chamber with pressures of $1.5 \sim 2 \times 10^{-4}$ Torr. In this chamber there were two cages made of multipole permanent magnets for surface plasma confinement and tungsten filaments as cathodes around the chamber wall. Thermal electrons emitted from the filaments collided with argon gases to generate a plasma. The chamber was separated into a driver region and a target one at the center by the separation grid kept at floating potential in order to control plasma parameters in these two regions independently. Typical plasma parameters in the experimental region were as follows: the electron density $n_e \approx 10^8 \text{ cm}^{-3}$

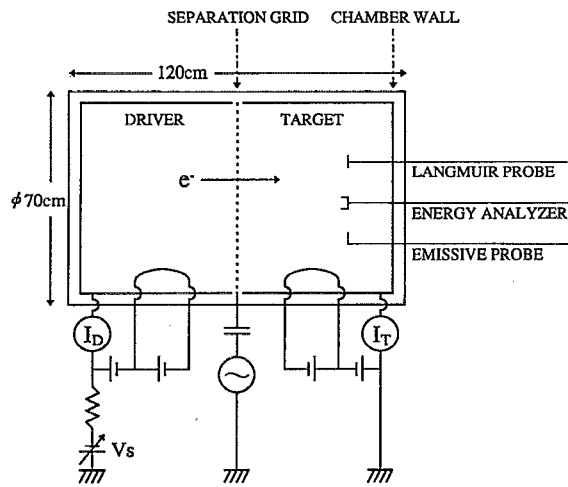


FIG. 1. Schematic diagram of the experimental apparatus.

and the electron temperature $T_e \approx 0.6$ eV. We generated an electron beam by the potential difference V_s between the driver and target plasma. The energy of the electron beam was ranged from 50 to 70 eV and was proportional to the potential difference V_s .

Plasma parameters and wave signals were measured with a plane Langmuir probe. The density of the electron beam was obtained by the integration of the measured I - V curve of the Langmuir probe. The energy distribution functions of electrons were obtained by the differentiation of the I - V curve of an energy analyzer. The space potential was measured with an emissive probe. The frequency spectrum was obtained from the observed wave signals of floating potential using a spectrum analyzer. Axial wave patterns were measured using a standard interferometric method, and the dispersion relation of waves was obtained from these wave patterns. The propagation direction of the waves was determined from the interferometric wave patterns measured when the phase of the reference signal was changed by a coaxial typed phase shifter. It is the first time to specify the propagation direction of the unstable waves using the phase shifter.

III. EXPERIMENTAL RESULTS AND DISCUSSION

O'Neil and Malmberg predicted that the mode characteristic of unstable waves in an electron beam plasma system changes depending on the energy distribution of an electron beam.¹⁸ To identify the mode of unstable waves excited by the injection of an electron beam, we measured the energy distribution function of electrons, in detail. Figures 2(a) and (b) show typical energy distribution functions of electrons, where Z denotes a distance from the separation grid. As shown in Fig. 2(a), the energy analyzer was placed in the upstream direction. This figure shows that there is an incident electron beam passing from the separation grid to the chamber wall. This electron beam attenuates only near the chamber wall. On the other hand, Fig. 2(b) is the result measured with the energy analyzer which was placed in the downstream direction. It is found that there is an electron

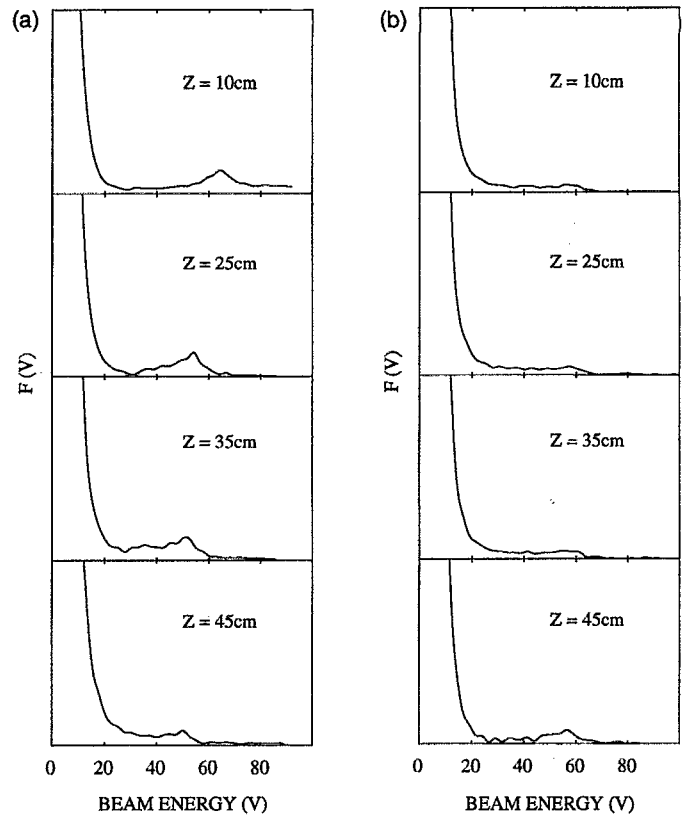


FIG. 2. Energy distribution functions $F(V)$ of electrons measured with an energy analyzer which is placed upstream direction (a), and downstream direction (b).

beam attenuating from the chamber wall to the separation grid, which indicates the existence of a reflected electron beam generated by the reflection of the incident electron beam near the chamber wall. Therefore, the reflected wave can be unstable due to the reflected electron beam.

We measured the frequency spectrum of spontaneously excited unstable waves with a spectrum analyzer. Figure 3 shows typical frequency spectra measured at the center of the experimental region for various I_T . Here I_T is the discharge current of the target plasma and is proportional to the plasma density in the experimental region. This figure shows that there are peaks around the electron plasma frequency. Note that the frequency corresponding to the strongest peak is discrete and becomes large as I_T increases.

When $I_T = 80$ mA, the electron plasma frequency, f_{pe} , calculated from the plasma density is estimated about 160 MHz. From Eq. (1) the frequency at which the growth rate of the electron beam plasma instability becomes maximum is given as

$$\omega_r \approx \omega_{pe} - \frac{1}{2^{4/3}} \omega_{pe} \left(\frac{n_b}{n_e} \right)^{1/3}. \quad (2)$$

In this experiment $n_b/n_e \approx 0.005$, so that $\omega_r/2\pi$ is about 149 MHz, which means that the strongest peak of 145 MHz shown in Fig. 3 corresponds to the frequency of the electron beam plasma instability with the maximum growth rate. We examined the frequency of the strongest peak of the unstable wave versus the plasma density when the energy of the elec-

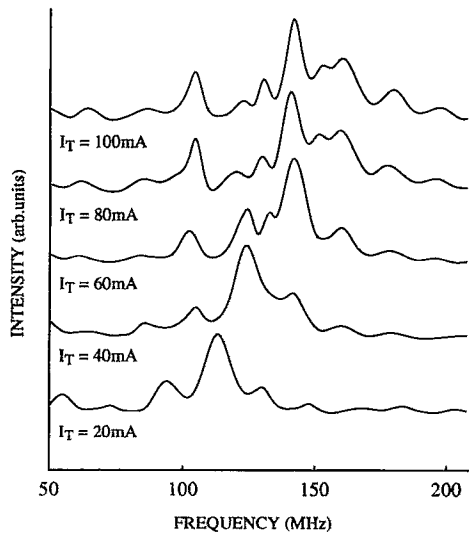


FIG. 3. Typical frequency spectra measured around the center of the experimental region ($Z=30$ cm), where $V_s=80$ V.

tron beam was varied, as shown in Fig. 4. Here a solid line denotes the frequency at which the growth rate of the wave excited by the electron beam plasma instability becomes maximum. This frequency was calculated from Eq. (2), where n_b/n_e was assumed to be 0.005 and constant. When an electron beam was injected into the plasma, the plasma density increased slightly, so that the increase in the plasma density was calibrated to estimate ω_r . Figure 4 shows that the frequency of the strongest peak of the spectrum becomes large as the plasma density increases although there are large scatters. This tendency agrees with that of the electron beam plasma instability. Furthermore, the dependence of the frequency on the energy of the electron beam qualitatively

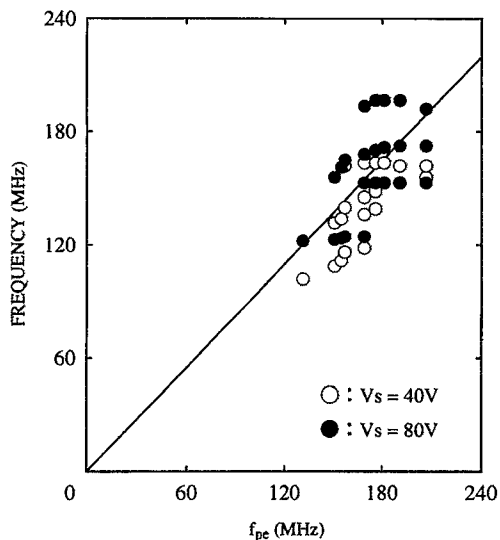


FIG. 4. Dependence of the frequency of unstable waves on the plasma density. A solid line denotes the frequency at which the growth rate of the electron beam plasma instability becomes maximum, where open circles and closed circles correspond to the experimental values for $V_s=40$ V and 80 V, respectively.

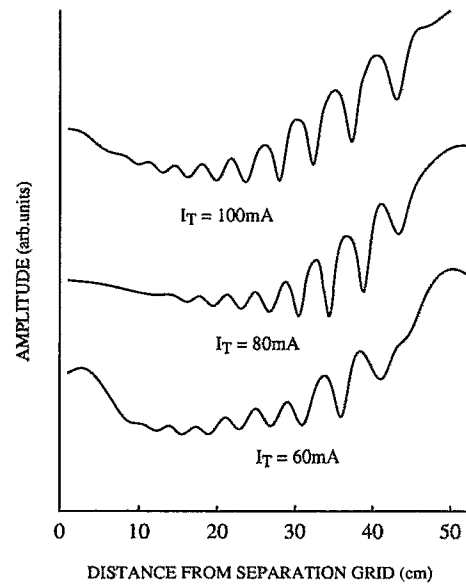


FIG. 5. Spatial profiles of the amplitude of the unstable wave measured with a spectrum analyzer, where $V_s=80$ V.

agreed with that of the linear theory. As seen in Fig. 3, fine structures were excited around the strongest peak. Thus, the frequencies measured around the electron plasma frequency distribute on the theoretical line due to the excitation of the fine structures, as shown in Fig. 4. These fine structures are considered to be caused by non-linear effects such as the parametric effect, as Kawabe¹⁵ pointed out.

When two electron beams flow against each other, the absolute instability may be excited.⁸ However, when there is a background plasma whose density is much higher than that of the electron beam like this experiment, the absolute instability is not excited. Thus, it is concluded that the instability observed here is not the absolute instability but the convective instability.

If the excited wave is a standing wave, the standing wave pattern can be ascertained with a spectrum analyzer. We measured axial profiles of the amplitude of the unstable waves for various I_T with the spectrum analyzer. Figure 5 shows that the unstable waves are found to be partly standing waves which are excited all over the experimental region. Assuming that the wavelength obtained from the standing wave patterns is half of the wavelength of the unstable waves, the product of the wavelength and the frequency of the waves is equal to the velocity of the electron beam.

The wave number of a standing wave is determined by the boundary condition, so that the frequency of unstable standing waves calculated from Eq. (1) becomes discrete. Because of the discrete frequency of the standing waves, the most unstable wave does not always have the frequency of the maximum growth rate.^{14,19} The unstable wave at a frequency corresponding to the available wave number is excited, and the frequency is closest to the frequency of the maximum growth rate. Thus, there was the slight difference between the observed frequency of the unstable wave, 145 MHz, and the numerically obtained frequency, 149 MHz. Figure 5 indicates that the wave number is kept nearly con-

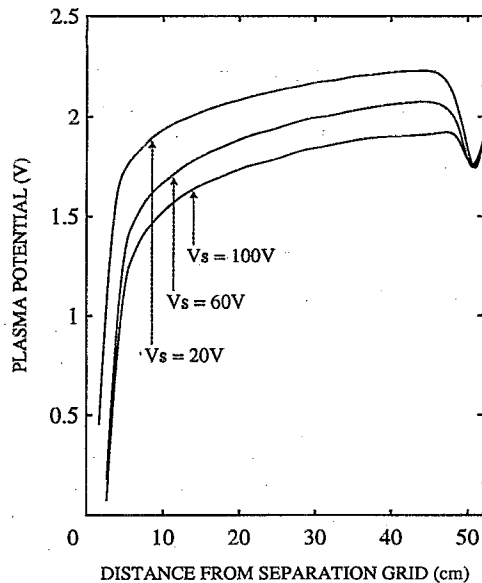


FIG. 6. Spatial profiles of the space potential at the experimental region measured with an emissive probe for different V_s .

stant when the electron density is varied. This characteristic agrees with that of standing waves which have discrete wave numbers. It is concluded from these results that the unstable wave observed here is mainly the standing wave excited by the electron beam plasma instability.

In order to specify the mechanism of the generation of the standing wave, we measured axial profiles of the space potential in the experimental region using an emissive probe. Typical potential profiles for different energies of the electron beam are shown in Fig. 6, which indicates that there is a potential well between the separation grid and the chamber wall. Since the height of the potential well is varied by the energy of the electron beam, this potential well is considered to be caused by the injection of the electron beam. The standing wave seems to be formed in this potential well. Matsunaga and Kato²⁰ solved the Poisson equation using linear approximation, and obtained the electrostatic potential profiles formed by the injection of an electron beam. According to them, the potential at the interior of plasma is lifted when the damping rate of the electron beam due to collisions increases. These profiles are similar to ours.

In order to obtain the dispersion relation and the propagation direction of the wave, we excited a propagating test wave and measured wave patterns by the interferometric method, as illustrated in Fig. 7. In this experiment the plasma density in the region where waves were excited was nearly constant, and the electron plasma frequency f_{pe} was about 160 MHz. Figure 7 shows that the waves with long wavelength ($\lambda \sim 7$ cm) are excited around the center of the experimental region. The amplitude of this wave is found to be nearly constant. On the other hand, the waves with short wavelength ($\lambda \sim 2$ cm) are excited near the chamber wall. Thus, these two waves are considered to be different modes from each other, because they have different wavelengths.

The waves with short wavelength were excited around the electron plasma frequency f_{pe} near the chamber wall, as

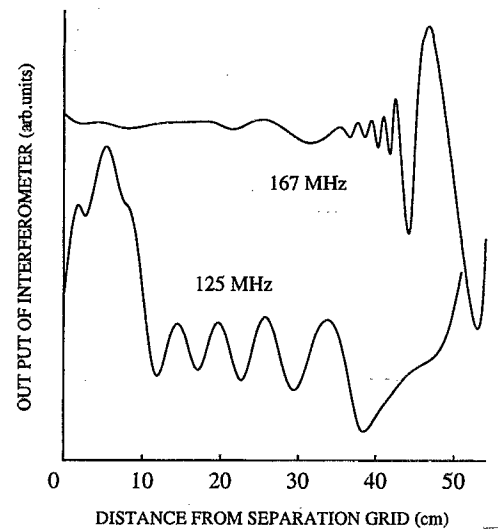


FIG. 7. Typical wave patterns near the electron plasma frequency f_{pe} measured using the standard interferometric method.

is also shown in Fig. 7. The dispersion relation obtained experimentally agrees well with the dispersion curve of the electron plasma wave. Also the Landau damping rate obtained experimentally agrees with that of the electron plasma wave. In order to determine whether this damping is caused by low frequency fluctuations or not, we measured the frequency spectrum around lower frequencies. However, the amplitude of the low frequency fluctuations was negligibly small. Therefore, the observed damping is specified to be the Landau damping. Furthermore, we measured the propagation direction of the waves using a phase shifter. It was found that the waves near the chamber wall propagate from the chamber wall to the center of the experimental region. These results mean that the wave excited near the chamber wall is the electron plasma wave propagating from the chamber wall to the center of the experimental region with Landau damping.

Here, we focus on the wave excited around the center of the experimental region. The frequency of the wave is lower than f_{pe} and agrees with that of the electron beam plasma instability. Figure 8 shows the dispersion relation obtained from the observed wave patterns, where a solid line denotes the theoretical dispersion curve of the electron beam plasma instability represented by Eq. (1). The experimentally obtained dispersion relation agrees with the branch of the beam mode of the dispersion curve. Propagation directions of test waves were measured using a phase shifter, as shown in Fig. 9. The phase of the reference signal of the lower wave patterns in these figures were delayed about $\pi/2$ against that of the upper wave patterns. Figures 9(a) and (b) show that there are two waves propagating in opposite directions from each other. The reason for which of the two waves is detected has not been understood. Figure 9(a) shows that there is a forward beam mode propagating from the separation grid to the chamber wall. Also, Fig. 9(b) shows a reflected beam mode propagating oppositely from the chamber wall to the separation grid. The former corresponds to the beam mode excited by the incident electron beam, and the latter to a reflected beam mode formed by the reflection of the forward beam

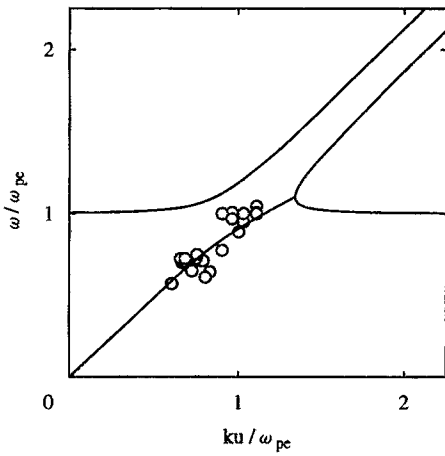


FIG. 8. Dispersion relation of test waves at the center of the experimental region. Solid lines denote the dispersion curve of the electron beam plasma instability.

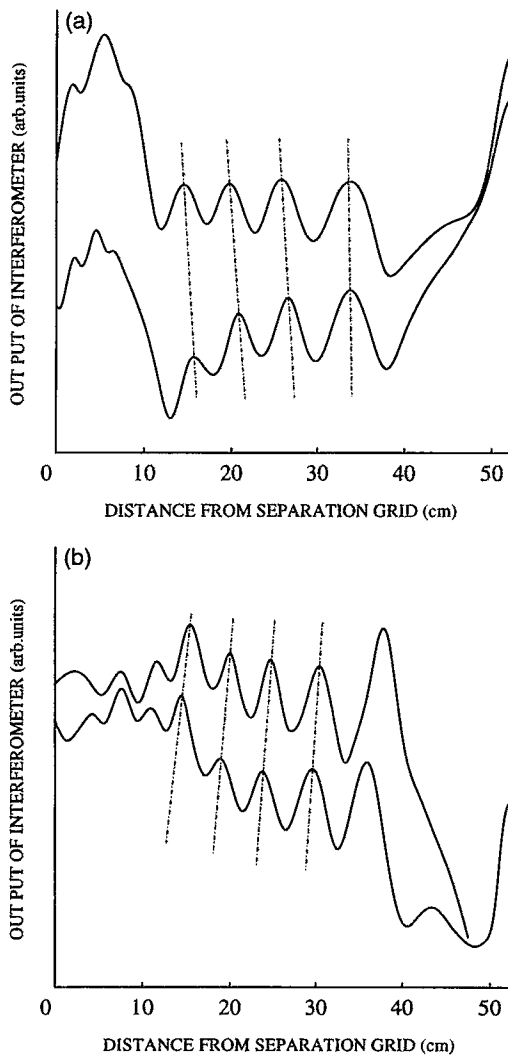


FIG. 9. Wave patterns of test waves when the phase of the reference signal is changed, where $V_s = 80$ V.

mode, respectively. These two beam modes did not damp, because the electron beam plasma instabilities were excited by the incident electron beam and reflected electron beam. Thus, the above results suggest that the standing wave is formed by superposing these beam modes propagating in opposite directions from each other. Furthermore, these results indicate that positive feedback necessary for standing waves is caused by the reflected beam mode propagating backward in the plasma. Roberson *et al.*^{16,17} measured the reflection coefficients of the electron plasma wave in an electron beam plasma system. In our experiment, the reflection coefficients of the beam mode were not measured, because we were interested in the excitation mechanism of standing waves in unstable systems.

Now, we specify the reason for the propagation of a reflected beam mode from the space potential well of the target plasma. It was found that as shown in Fig. 6, there are negative potential drops in front of the separation grid and the anode with permanent magnets near the chamber wall. It seems that this negative potential drop in front of the anode plays a role of the boundary. Then the forward beam mode was reflected at this point, and propagated as the reflected beam mode in the opposite direction. Thus, the forward and reflected beam modes were observed in this potential well produced by the injection of the electron beam. Therefore the standing wave is considered to be formed in this potential well.

Usually a standing wave is observed with a spectrum analyzer and a traveling wave is observed by the interferometric method with a phase shifter. In this experiment, both the standing wave and the traveling wave were observed simultaneously. This is explained as follows. The potential ϕ of the forward wave and the reflected wave are assumed as $\cos(kx - \omega t)$ and $\Gamma \cos(kx + \omega t)$ respectively, where k and ω are the wave number and frequency of waves, respectively, and Γ is the reflection coefficient. These two waves are superposed and rewritten in two ways :

$$\begin{aligned} \phi &= \Gamma \cos(kx - \omega t) + \Gamma \cos(kx + \omega t) + (1 - \Gamma) \\ &\quad \times \cos(kx - \omega t) \\ &= 2\Gamma \cos kx \cos \omega t + (1 - \Gamma)\cos(kx - \omega t), \end{aligned} \quad (3)$$

$$\begin{aligned} \phi &= \cos(kx - \omega t) + \cos(kx + \omega t) + (\Gamma - 1)\cos(kx + \omega t) \\ &= 2 \cos kx \cos \omega t + (\Gamma - 1)\cos(kx + \omega t). \end{aligned} \quad (4)$$

When $\Gamma < 1$, the amplitude of a reflected wave is smaller than that of a forward wave, Eq. (3) can be applied. Then both a standing wave and a forward traveling wave are obtained. Also when $\Gamma > 1$, the amplitude of a reflected wave is larger than that of a forward wave, Eq. (4) can be used. Thus both a standing wave and a reflected traveling wave coexist. These results agree with our experimental facts that both the standing wave and traveling wave were observed.

IV. CONCLUSION

The excitation mechanism of standing waves observed in an electron beam plasma system was experimentally studied. There existed an incident electron beam and a reflected

electron beam in the electron beam plasma system. The standing waves were excited around the center of the experimental region by the electron beam plasma instability. Test waves were propagated and the dispersion relation was measured. It was found that both a forward beam mode and a reflected beam mode propagate in opposite directions from each other in the potential well caused by an electron beam injection. As a result, the standing wave was produced by superposing these beam modes.

ACKNOWLEDGMENTS

The authors would like to acknowledge the useful discussions with Professor R. Sugaya and Professor T. Kato.

¹D. Bohm and E. P. Gross, *Phys. Rev.* **75**, 1851 (1949).

²H. Derfler and T. C. Simonen, *Phys. Rev. Lett.* **17**, 172 (1966).

³C. W. Roberson, K.W. Gentle, and P. Nielsen, *Phys. Rev. Lett.* **26**, 226 (1971).

⁴K. W. Gentle and C. W. Roberson, *Phys. Fluids* **14**, 2780 (1971).

⁵J. H. Malmberg and C. B. Wharton, *Phys. Fluids* **12**, 2600 (1969).

⁶D. A. Hartmann, C. F. Driscoll, T. M. O'Neil, and V. D. Shapiro, *Phys. Plasmas* **2**, 654 (1995).

⁷Y. Kawai, Y. Nakamura, T. Itoh, T. Hara, and T. Kawabe, *J. Phys. Soc. Jpn.* **38**, 876 (1975).

⁸R. J. Briggs, *Electron-Stream Interaction with Plasmas* (MIT Press, Cambridge, MA, 1964).

⁹M. Seidl, W. Carr, D. Boyd, and R. Jones, *Phys. Fluids* **19**, 78 (1976).

¹⁰M. J. Kofoed, *Phys. Rev. Lett.* **4**, 556 (1960).

¹¹M. J. Kofoed, *Phys. Fluids* **5**, 712 (1962).

¹²D. A. Dunn, W. Nichparenko, J. E. Simpson, and K. I. Thomassen, *J. Appl. Phys.* **30**, 3237 (1965).

¹³D. H. Looney and S. C. Brown, *Phys. Rev.* **93**, 965 (1954).

¹⁴M. Sumi, *J. Phys. Soc. Jpn.* **14**, 1093 (1959).

¹⁵T. Kawabe, *J. Phys. Soc. Jpn.* **21**, 2704 (1966).

¹⁶C. W. Roberson, A. S. Ratner, and J. L. Hirshfield, *Phys. Rev. Lett.* **31**, 1041 (1973).

¹⁷C. W. Roberson and J. Fukai, *J. Appl. Phys.* **45**, 2489 (1974).

¹⁸T. M. O'Neil and J. H. Malmberg, *Phys. Fluids* **7**, 1534 (1964).

¹⁹M. Sumi, *J. Phys. Soc. Jpn.* **15**, 120 (1960).

²⁰Y. Matsunaga and T. Kato, *J. Phys. Soc. Jpn.* **63**, 4396 (1994).